Available online at www.sciencedirect.com

SCIENCE DIRECT®

ELSEVIER

International Journal of Mass Spectrometry 252 (2006) 166–172

International Journal of Mass Spectrometry

www.elsevier.com/locate/ijms

Metastable dissociation and kinetic energy release of helium clusters upon electron impact ionization

S. Feil[a], K. Gluch[b], S. Denifl[a], F. Zappa[a], O. Echt[c,1], P. Scheier[a], T.D. Märk[a,*]

[a] *Institut für Ionenphysik, Leopold Franzens Universität, A-6020 Innsbruck, Austria*
[b] *Institute of Physics, Maria Curie-Sklodowska University, 20-031 Lublin, Poland*
[c] *Department of Physics, University of New Hampshire, Durham, NH 03824, USA*

Received 16 October 2005; received in revised form 16 January 2006; accepted 16 January 2006
Available online 20 March 2006

Abstract

Neutral helium clusters, formed in a supersonic beam, are subjected to electron impact ionization. We report resolved size distributions of cations of size $n \leq 300$. The distributions show the well established anomalies at $n = 10$ and 14, but none for larger sizes. MIKE scans of the cluster ions confirm the anomalies at $n = 10$ and 14, and another one at $n = 7$. Surprisingly broad distributions of fragment ions are observed for parent sizes $15 \leq n \leq 30$. These findings are attributed to radiative heating. The kinetic energy released upon loss of one helium atom (KER) has been measured. The values drop below 1 meV for $n > 20$. Neither the metastable fragment distribution nor the KER data provide evidence for the release of large, quantized energies that one would expect for relaxation of any long-lived vibronic states of the ionic core.

Keywords: Electron impact ionization; Mass spectrometry; Metastable decay; MIKE scan; Kinetic energy release

1. Introduction

Since the discovery of condensation in a helium nozzle expansion in 1961 [1], the investigation of helium clusters has been a focus of cluster research. One major impetus has been the extreme quantum nature of these clusters, paralleled by only one other system, namely hydrogen clusters [2]. The occurrence of superfluidity in ^4He_n clusters containing as few as $n = 60$ atoms has recently been established by theory and experiment [3,4]. Another reason that has made helium droplets a "hot topic" is their use as nano-reactor to study ion-molecule reactions [5], or for spectroscopy of embedded molecules at subkelvin temperatures [6]. Yet another reason for the unabated interest is the formation of bubbles around electrons and electronically excited helium atoms within or at the surface of helium clusters [2,7,8].

The breadth and ingenuity of technical approaches taken in the study of helium clusters is breathtaking. Even though helium clusters are much more difficult to generate than other weakly bound elemental clusters, helium is the only system for which the size distribution of *neutral* clusters has been measured over a wide range by a technique that is essentially non-destructive, namely by diffraction off nano-structured grids [9]. The technique has recently revealed "magic numbers", i.e., local enhancements in the neutral cluster size distribution, at $n = 10$–11, 14, 22, 26–27 and 44 atoms [10].

On the other hand, some of the more conventional techniques that rely heavily on mass spectrometry have not yet been applied. There has been continued interest in long-lived electronic excitations in neutral and charged helium clusters since the pioneering work by Gspann and coworkers [11,12] who reported that electron impact ionization of large helium clusters containing roughly 10^6 or more atoms leads to the emission of charged miniclusters of less than 100 atoms (for more recent work, see refs. [13,14], and references in the excellent review by Northby [15]). Metastable states in much smaller cluster ions could exist as well, and they could be explored with unit size resolution. Nevertheless, we are aware of only one such study, pertaining to He_4^+ [16].

In this work, we analyze metastable reactions of small He_n^+ cations. We present fully resolved size distributions that extend

---

[*] Corresponding author. Also Adjunct Professor at Department of Plasma Physics, Comenius University, SK-84248 Bratislava, Slovak Republic.

E-mail addresses: olof.echt@unh.edu (O. Echt), tilmann.maerk@uibk.ac.at (T.D. Märk).

[1] Also Guest Professor at the University of Innsbruck.

1387-3806/$ – see front matter © 2006 Elsevier B.V. All rights reserved.
doi:10.1016/j.ijms.2006.01.055

to $n = 300$, way beyond the range of previous studies [17–22]. In contrast to some earlier studies [19,21], we find that the size distribution of cluster ions is void of any intensity anomalies beyond $n = 14$.

The probability of metastable decay of $He_n{}^+$ into $He_f{}^+$ is analyzed by the MIKE techniques. Surprisingly, the probability P_f does not level off until very small fragment sizes, around $f = 5$, are reached. P_f reflects the well known magic numbers of the direct mass spectra at $n = 7$, 10 and 14, but there is no evidence for spontaneous release of a large, quantized amount of energy that one would expect if electronic or vibrational relaxation of an excited species such as $He_2{}^{+*}$ would happen on the experimental time scale of about 10 μs. The unusually broad distributions of evaporations that we observe is attributed to radiative heating of the cold cluster ions. Lastly, we report the kinetic energy released upon He evaporation from $He_n{}^+$ for $n \leq 27$.

2. Experiment

Details of the experimental setup and data analysis have been published elsewhere [23]. The apparatus consists of a high resolution double focusing mass spectrometer (Varian MAT CH5-DF) of reversed Nier-Johnson type B-E1 geometry combined with a second electrostatic analyzer E2. Neutral clusters are produced by expanding helium from a stagnation chamber at $T_0 = 9$ K and a pressure of 20 bar or less through a pin-hole nozzle (5 μm diameter) into vacuum. The clusters are ionized by an electron beam of 100 eV; the pressure in this region is 2×10^{-7} mbar. Ensuing cations are extracted by a weak electric field and accelerated through a potential drop of $U_{ac} = 3$ kV into the spectrometer. They pass through the first field-free region (ff1, length 61 cm), are momentum-analyzed by a magnetic sector field B, enter a second field-free region (ff2, length 33.3 cm), pass through a 90° electric sector field ($E1$) and are finally detected by a channeltron-type electron multiplier. The metastable window (ff2) is $10.6 \leq t \leq 13.5$ μs for $He_{10}{}^+$ parent ions; for other cluster ions the window scales as $\sqrt{n}$. The second electric sector field is not used in the present work.

Mass-analyzed ion kinetic energy (MIKE) spectra of parent ions $He_n{}^+$ that undergo spontaneous decay in ff2,

$$He_n{}^+ \rightarrow He_f{}^+ + (n - f)\,He \qquad (1)$$

are monitored as follows: the magnet is tuned to transmit the parent ion while the sector field voltage U of E1 is scanned [24]. If U_p denotes the voltage required to transmit a stable parent ion ($U_p \approx 511$ V in our system), then the electric sector will transmit fragment ions $He_f{}^+$ formed in ff2 if the sector field voltage is set to

$$U_f = \frac{f}{n} U_p. \qquad (2)$$

So far we have ignored the fact that the parent ions will have a finite kinetic energy distribution that gives rise to a finite width and characteristic peak shape in the MIKE scan. Any kinetic energy release (KER) in reaction (1) will modify the peak shape of the fragment ions. The shape will be Gaussian if the kinetic energy release follows a Maxwell–Boltzmann distribution [25] and if its average value $\bar{\varepsilon}$ is relatively small such that neither the finite length of the exit slit nor the finite size of the detector give rise to discrimination against ions that are emitted with large z-components, i.e., along the direction of the slit. The average kinetic energy $\bar{\varepsilon}$ may then be extracted from the width ΔU of the fragment ion peak, measured at full-width-at-half-maximum,

$$\bar{\varepsilon} = 2.16 \frac{n^2 U_{ac}}{16 f (n - f)} \left(\frac{\Delta U}{U_p} \right)^2 \qquad (3)$$

The width ΔU has first to be corrected for the finite width of the parent ion by deconvoluting the fragment ion signal with the parent ion signal. As discussed elsewhere [23,25], one may deduce the binding energy of the cluster ions from their average kinetic energy release, provided the reaction is statistical.

Another quantity of interest is the metastable fraction of a fragment ion. It is defined as

$$MF_f = \frac{I_f}{I_n + I_f} \qquad (4)$$

where I_f and I_n are the intensities of the fragment and parent ions, respectively.

3. Results and discussion

3.1. Mass spectra

Fig. 1 displays a mass spectrum of helium cluster ions (note the logarithmic intensity scale). The upper panel shows cluster ions up to $n = 150$, the lower panel continues to $n = 300$. For small sizes ($n \leq 14$) we observe reproducible structure in the intensity distribution; this will be discussed further below. In contrast, any local anomalies or smooth undulations that appear for larger clusters are caused by temporary fluctuations of the neutral cluster beam intensity, minor variations of the nozzle temperature or occasional partial clogging of the nozzle by impurities in the helium gas. In particular, we have confirmed that the prominent minimum in Fig. 1 around $n \approx 75$ is not reproducible. Below $n \approx 100$, background ions visibly contribute to the spectrum. The narrowly spaced background peaks are not graphically resolved in Fig. 1; they give rise to the black smudge in the bottom left of the upper panel.

Gspann and coworkers have suggested that large helium clusters ($n \approx 10^6$) will, upon ionization, expel charged "miniclusters" with an average size of 68 atoms [12]. Another mechanism that has been suggested to produce cluster cations in this size range is double ionization: Farnik et al. have estimated that doubly charged helium clusters of size $n \leq 2 \times 10^5$ will spontaneously undergo strongly asymmetric fission [14]. According to the model, the smaller fragment ion will contain some ≈50 atoms. The energy of the electron beam in our experiment is 100 eV and the electron current is high, hence the formation of doubly charged clusters is quite likely. Nevertheless, the spectrum in Fig. 1 provides no evidence for the proposed ejection of small $He_n{}^+$ from $He_x{}^{2+}$ or large $He_x{}^+$.

We now turn our attention to small cluster ions. The upper panel of Fig. 2 presents a histogram of small helium clusters

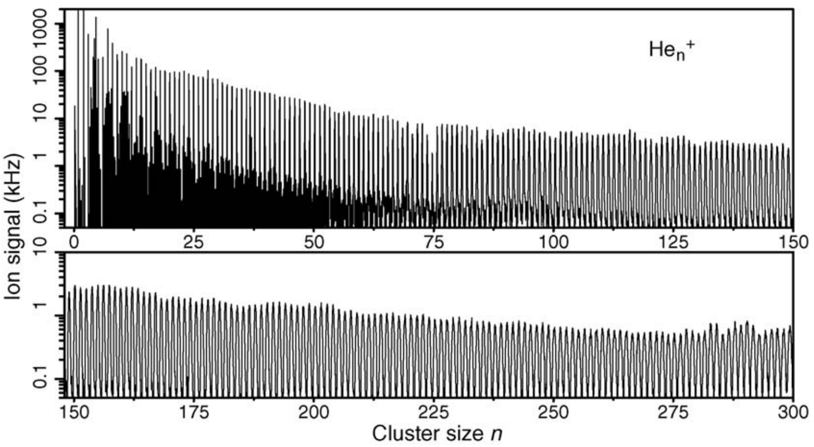

Fig. 1. Mass spectrum of helium cluster cations up to size $n = 300$. The local intensity anomalies observed for very small cluster ions, $n \leq 14$, are reproducible; all other anomalies are caused by fluctuations of the helium expansion temperature, nozzle instabilities or contributions from residual gas.

($n \leq 32$). The background contribution has been measured separately, with the helium beam off, and subtracted from the spectrum shown. Two reproducible maxima at $n = 10$ and 14, previously reported by other investigators [17–22], are clearly discernible while another anomaly at $n = 7$, reported before by some groups [17,20,22], is not. This anomaly has been controversial because it might be caused by N_2 impurities. The metastable spectrum of He_{21}^+, plotted in the bottom panel of Fig. 2 versus the size of the fragment ions (see Section 3.2 for details), does indeed provide unambiguous evidence for an anomaly at $n = 7$, in addition to the ones at $n = 10$ and 14. However, Fig. 2 provides no basis for the claim of anomalies at $n = 22$ [21], 23 [17], 30 [17,21], or 57 and 77 [21]. Buchenau et al. also reported various anomalies in this size range, for example, $n = 4$, 13, 16, 21, 24, 28 and 31, depending on the expansion conditions [19]. However, they cautioned that impurities may have caused some or all of these anomalies.

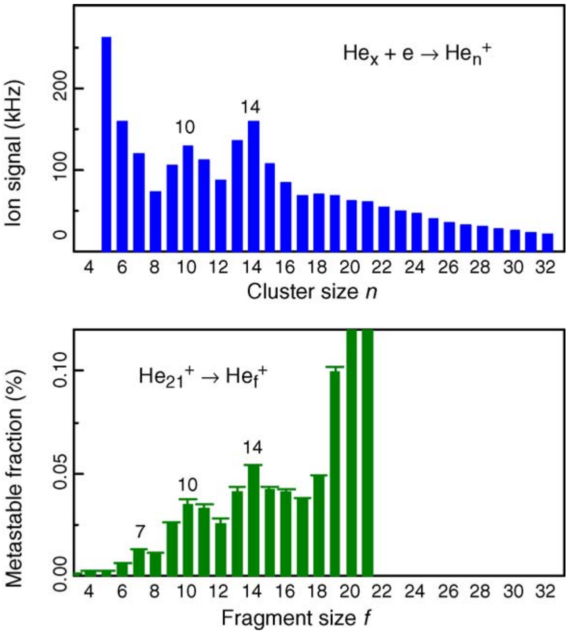

Fig. 2. (Top panel) Mass spectrum of small helium cluster ions, corrected for contributions from residual gas. (Bottom panel) Probability for metastable formation of He_f^+ from He_{21}^+ vs. fragment size f. Error bars indicate uncertainties based on three separate measurements. Note the similarity of intensity anomalies in the two spectra.

The restriction of anomalies in size distributions of He_n^+ to small values of n contrasts with observations for various other van der Waals cluster ions. For example, intensity anomalies in spectra of Ne_n^+ and Ar_n^+ formed by electron impact ionization of pre-formed clusters are rather weak and/or uncommon below $n \approx 55$ where the second icosahedral shell is completed [26–28]. CO_n^+ and $(CH_4)_n^+$ show no or only very weak anomalies until the third icosahedral shell closes at $n = 147$ [29,30].

A possible explanation for the absence of anomalies for $n > 14$ in He_n^+ might be thought to be a transition from solid to liquid with increasing n. Clusters of the heavier inert gases will, upon evaporative cooling, quickly freeze into solids; this will hold for neutral as well as charged clusters [31,32]. Helium is different. At ambient pressures and below, neutral helium clusters will be, like bulk helium, liquid. The ionic core of a helium cluster ion will be solid-like, but the outer shells will be liquid. Liquid clusters do not exhibit any “magic numbers” related to particularly favorable geometric structures [33], although they may possibly reveal magic numbers due to the quantization of the excitation spectrum [10], or structure in the electronic level density (see [34] and references therein). However, the cluster ions investigated in the present study may be too small to exhibit liquid layers. A positive ion in condensed helium is surrounded by a rigid shell containing about 30–50 He atoms (see [6] and references therein). The structure of somewhat larger cluster ions has, to our knowledge, not yet been determined directly.

3.2. Metastable decay

Eq. (4) defines the so-called metastable fractions of cluster ions which are a measure of metastable dissociation in a particular channel, from parent size n into fragment size f Fig. 3 presents the metastable fractions for dissociation of He_n^+ into He_{n-1}^+ as a function of n. Two separate measurements were recorded and combined for $n \leq 15$; the statistical errors shown in Fig. 3 were

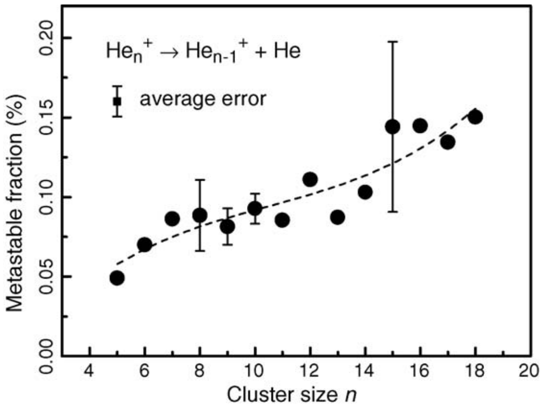

Fig. 3. Probability for metastable loss of one helium atom from He_n^+ vs. size n. Error bars are determined from two separate measurements up to $n \leq 15$; the average of these errors is also indicated. The dashed line is drawn to guide the eye.

calculated from the differences between the two sets. The error bars are found to fluctuate widely with n because of the small sample size. We also display the average of all errors which is a more realistic assessment of the statistical quality of the data. A gradual increase of the metastable fraction with increasing n is observed, as expected for an evaporative ensemble [35]. The statistical fluctuations in Fig. 3 mask any small anomalies that one may expect based on the data shown in Figs. 1 and 2.

Although the data in Fig. 3 display the usual trend, i.e., an increase in the metastable fractions with increasing size n, the observed values are an order of magnitude smaller than one would expect for the specific time window in our experiments. We have applied the formalism developed by Barran et al. [36] to fit a Gspann factor G (defined as the logarithm of A/k where A is the pre-exponential in the Arrhenius expression for the decay rate constant, and k the value of the rate constant, $k \approx t^{-1}$, where t is the time elapsed since the formation of the ensemble) to our data. We have assumed constant dissociation energies D_n for He_n^+ which should be an acceptable assumption for the larger clusters in our study, $n > 10$. If we use the classical value $C = (3n - 6)k_B$ for the vibrational heat capacities we obtain $G = 87$. The value is physically unreasonable. If, on the other hand, we assume the usual value of $G \approx 25$ [37], we predict metastable fractions that are at least an order of magnitude larger than observed.

The disagreement between the metastable fractions measured for He_n^+ and the ones observed for other elemental cluster ions most likely stems from the quantum properties of helium. True, the thermal and kinetic properties of bulk helium near 4.2 K are not unlike those of the other inert gas liquids near their respective boiling points [38]. In particular, its molar heat capacity is not much less than the classical equipartition value. However, whereas conventional cluster systems will cool by evaporation to approximately 40% of their respective boiling points [39], helium droplets will cool much more strongly to 0.4 K [4] where their heat capacity is orders of magnitude below the classical value [38]. The presence of a charge will increase the binding in the ion core (according to a spectroscopic study by Haberland et al. the charge will be localized either on a trimer or a tetramer [40]), but somewhat larger cluster ions are still expected to cool to below 1 K. Unfortunately, the vibrational excitation spectrum of helium cluster ions is not available, hence we cannot give a quantitative estimate of their heat capacities and the effect on the metastable fractions.

The bottom panel in Fig. 2 displays the probability for He_{21}^+ to decay into He_f^+ versus fragment size f. These data are obtained from an extended MIKE scan in the second field-free region of the mass spectrometer, varying the electric sector field voltage from the value that permits transmission of the stable parent all the way to zero. The relative size of the fragment, f/n, equals the relative value of the electric sector field voltage at which a metastable ion is observed, see. Eq. (2). In Fig. 2, we show the average of three MIKE scans for He_{21}^+; the error bars represent the uncertainties determined from the standard deviations. As mentioned in Section 3.1, this spectrum provides clear evidence for the special nature of He_7^+, He_{10}^+ and He_{14}^+. Additional evidence comes from the observation of identical anomalies in decay spectra recorded for parents other than He_{21}^+.

It is surprising to observe metastable decay of He_{21}^+ into fragment ions as small as He_5^+. The energy required for evaporation of 16 atoms cannot possibly be stored in vibrational modes of the cluster ion. Such a large amount of energy would result in a rate constant greatly exceeding the inverse experimental time scale. However, there are several other mechanism that could give rise to such a fragment ion distribution:

(1) Non-statistical decay, namely the relaxation of energy that is not yet randomized in the cluster ion. A fingerprint of this channel would be the spontaneous ejection of several cluster constituents. Such a phenomenon happens, for example, from vibrational relaxation of nitrogen molecules in $(N_2)_n^+$ [41–43], and exciton decay in argon and neon cluster ions [44,45]. For small helium cluster ions, release of just one vibrational quantum of the ionic core would suffice to eject all weakly bound atoms, thus the decay would predominantly produce a very small fragment ion. This is not what we observe.

    Long-lived vibrational states in He_n^+ are, indeed, unlikely. A quantum molecular dynamics study by Gianturco and coworkers suggests that charge localization and collisional quenching of vibrationally excited He_2^+ will occur on the order of picoseconds [46], although ejection of the excited molecular ion is a competing reaction [47]. On the other hand, metastable electronically excited atomic and molecular states are a striking, widely studied feature of large neutral and charged helium clusters (see the review by Northby [15]). Less is known about metastable states in small He_n^+. von Issendorf et al. have demonstrated that He_4^+, which is a prominent fragment ion if very large clusters are excited by electron impact [13], is electronically excited with a lifetime of the order 10^{-4} s [16]. Some 10% of the He_5^+ ensemble was reported to be electronically excited, too. However, our MIKE spectra do not provide any evidence for a metastable reaction that would release a distinct energy greatly exceeding the binding energy of the ligands

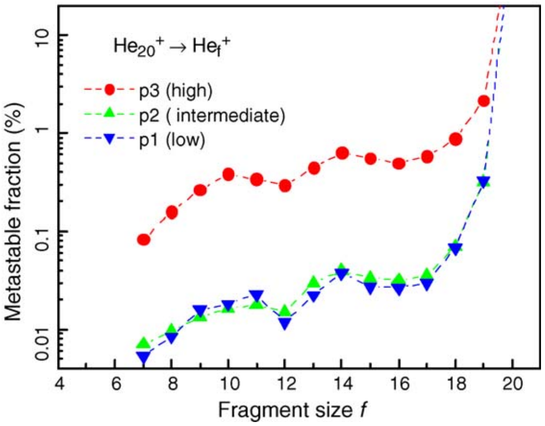

Fig. 4. Probability for metastable formation of He_f^+ from He_{20}^+ vs. fragment size *f* for three different pressures in the second field-free region where the reaction is measured. The pressures differ by approximately two orders of magnitude between adjacent curves with $p_3 \gg p_2 \gg p_1 \approx 10^{-8}$ mbar. The close similarity of the two curves recorded for the two lower pressures suggests negligible contributions from collision induced processes at $p_1 \approx 10^{-8}$ mbar.

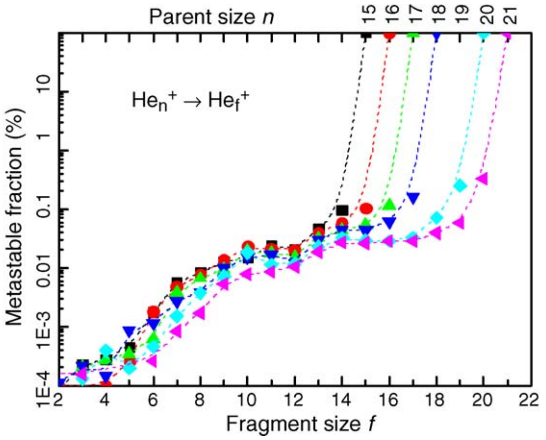

Fig. 5. Probability for metastable formation of He_f^+ from He_n^+ vs. fragment size *f* for various parent ions. The parent size ($15 \leq n \leq 21$) is indicated along the top abscissa.

($D \approx 20$ meV for He_5^+ [48] and much less for larger cluster ions).

(2) Alternatively, dissociation may be induced by collisions of the ions with the background gas. The pressure in the field-free region is about 10^{-8} mbar, rendering this process unlikely. Nevertheless, to remove any doubt we have performed MIKE scans for He_{20}^+ for three different pressures in the field-free drift tube, namely $p_1 \approx 10^{-8}$ mbar (base pressure), $p_2 \approx 10^{-6}$ mbar and $p_3 \approx 10^{-4}$ mbar. Fig. 4 shows the results of these measurements. The data are essentially identical for p_1 and p_2 only for p_3 do we have a clear contribution from collisions.

The negligible difference between the p_1 and p_2 data proves that collisions do not contribute to the observed fragment ions of He_{20}^+ at the lowest pressure, $p_1 \approx 10^{-8}$ mbar.

(3) Another mechanism that can transfer energy to the cluster ions is radiation. The more commonly encountered process is the reverse, namely radiative cooling which has been discussed, for example, by Dunbar for molecules [49] and by Hansen and Campbell for atomic clusters [50]. In the present study, the helium cluster ions will quickly cool by evaporation to very low temperatures, depending on the binding energy of outer ligands and, hence, the cluster size (neutral helium clusters will cool to about 0.4 K). The absorption of radiation from the ambient black body radiation will then cause ejection of atoms. Bondybey and coworkers were among the first to report such an effect, for protonated water clusters [51]. A dissociation rate of the order $1\,s^{-1}$ was reported for small water cluster ions. To estimate the expected rate for small helium cluster ions, one would need to know their IR absorption spectrum which, to the best of our knowledge, is not available (Haberland and coworkers have reported the absorption spectrum of small helium cluster ions in the UV [40], but the large absorption strength in this energy range will hardly contribute to radiative heating at 300 K). For a rough estimate we note that the dissociation energy of cluster ions converge, for not too small a size, to the bulk vaporization energy which is three orders of magnitude smaller for helium than for water. This would amplify the dissociation rate of He_n^+ to $10^3\,s^{-1}$. The data in Fig. 4 (for low pressure, integrated over all fragments of size $n < 18$) show a decay probability of $\approx 2 \times 10^{-3}$. The time window of the measurement is 4.1 μs, hence the decay rate is $500\,s^{-1}$ in (probably fortuitous) agreement with the scaled water cluster data. Note that there is a qualitative difference between radiative dissociation of water and helium cluster ions: the former require absorption of several photons (a typical photon energy at 300 K is 0.1 eV), thus a size-selected cluster ion will, with increasing time, slowly shrink in size as indeed observed in the experiment [51]. In contrast, the size distribution of fragment ions from He_n^+ will always be broad because a single photon will suffice to emit several atoms, and the black-body spectrum covers a large energy range.

Further support for this interpretation comes from the MIKE scans for parents ions $15 \leq n \leq 21$, shown in Fig. 5. The parent size is indicated along the upper abscissa. All curves show the same characteristic shape. The small "metastable" fractions ("radiation induced fractions" would be more appropriate) suggests that, on the time scale of the experiment, no more that one photon is observed. Larger clusters lose, on average, more atoms because their dissociation energies are smaller. On the other hand, the distributions level off below $n = 7$ because the dissociation energy increases with decreasing *n*.

3.3. Kinetic energy release

The upper panel of Fig. 6 presents a MIKE scan of He_6^+. The peak to the right at a sector voltage of 511 V is the parent ion. To the left, centered at 426 V ($426 = 511 \times 5/6$, see Eq. (2)), one finds the fragment ion He_5^+; its intensity has been multiplied by a factor 5000 to make it visible. Under the fragment ion peak we display the properly scaled parent ion peak; it is clear that the fragment ion peak is broadened due to the kinetic

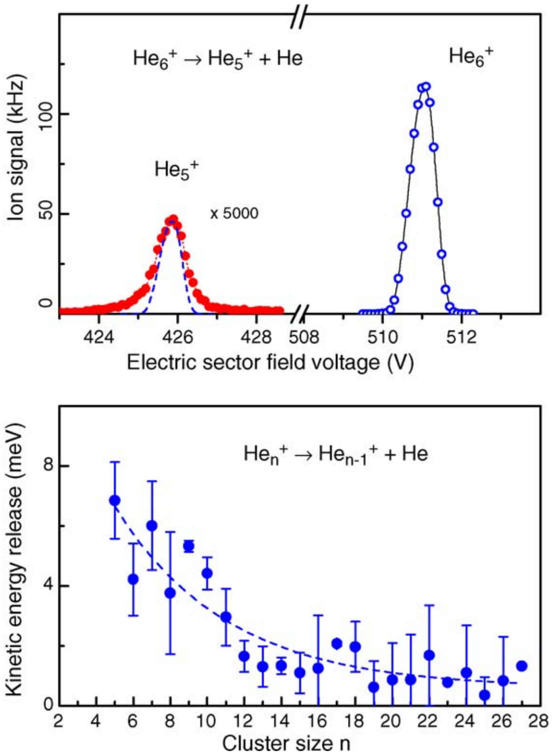

Fig. 6. (Top panel) MIKE scan of the parent ion He_6^+ and its metastable fragment He_5^+ (enhanced by a factor 5000). Lines through the data points are drawn to guide the eye. The dashed line under the fragment ion peak indicates the width of the parent ion peak, scaled to the position of the fragment ion. The difference between the two peaks shown at 426 V measures the kinetic energy release of the reaction. (Bottom panel) Average kinetic energy released upon loss of one atom from He_n^+. Error bars are deduced from separate measurements. The line is drawn to guide the eye.

energy released in the reaction. The relatively small broadening and the very low ion intensity make it difficult to obtain accurate values for the average kinetic energy release $\bar{\varepsilon}$. Moreover, most of the parent ions in this size range contain some contributions from background gas. Although the background can be, and has been, removed whenever necessary (except for the data shown in Fig. 1), highest accuracy is achieved for He_6^+ because no hydrocarbons or inorganic molecules contribute to the ion peak at 24 u. We have repeated MIKE scans of individual sizes, $5 \leq n \leq 27$, in up to eight separate runs. Uncertainties were estimated from these data; they are displayed as error bars. Still, the possible effect of contaminants is difficult to assess in KER measurements (see [23] for a detailed discussion) and our results for the KER should be taken with a grain of salt.

The lower panel of Fig. 6 displays the average KER values for He_n^+ cluster ions. The values are rather larger, especially for $n \leq 10$. It is instructive to compare these values with previously reported values for neon cluster cations [52]. For the smallest size investigated, $7 \leq n \leq 10$, the KERs of Ne_n^+ were somewhat less than our current results for helium. The application of finite heat bath theory [53] or other statistical methods that link the KER to the transition state temperature and thus the stability of the ions [25,54], would then suggest that the dissociation energies $D_n = E_n - E_{n-1}$ of small He_n^+ are larger than those of Ne_n^+. This result is implausible because the heat of vaporization of bulk neon exceeds that of helium by an order of magnitude. Although the disparity is not necessarily as large for small cluster ions, thermochemical data reported by Hiraoka and Mori show that the heat of vaporization of He_5^+, the largest helium cluster ion covered in their study, is 60% below that of Ne_5^+ [48]. We conclude that our KER values shown in Fig. 6 are only upper estimates. In a recent study of KER values of neon, argon and krypton cluster ions we had used a three sector field mass spectrometer [23]; those data were much more accurate than data recorded with a double focusing mass spectrometer. In the present study, the low intensity of the metastable decay precluded the use of the triple instrument; thus limiting the accuracy of our data for helium.

Furthermore, the conversion of kinetic energy release into dissociation energies involves the heat capacities. As we have seen in Section 3.2, these are not adequately approximated by the equipartition values; hence a more complete analysis of our KER data cannot be done without knowledge of the excitation spectrum of small helium cluster ions.

4. Conclusion

We have presented fully resolved size distributions of He_n^+ for sizes $n \leq 300$. The spectrum argues against the occurrence of magic numbers for $n \geq 14$; the findings are consistent with the notion that larger helium cluster ions are liquid-like. MIKE scans have been recorded for various parent ions. The metastable fractions for loss of one atom from He_n^+ were presented for $5 \leq n \leq 18$. The fractions are roughly a factor 10 smaller than expected for an evaporative ensemble of clusters. This discrepancy is attributed to the strong reduction of the heat capacity in cold helium cluster ions. A small fraction of the He_n^+ ions of size $15 \leq n \leq 30$ are observed to spontaneously lose most of their atoms, on a time scale of 10 μs after ion formation. Collision induced fragmentation or relaxation of long-lived excited states have been excluded as possibly mechanisms. Instead we suggest that the spontaneous dissociation occurs subsequent to absorption of a photon from the ambient radiation field. Finally, we have reported kinetic energy release data. Unfortunately, the unknown heat capacities and the limited accuracy of the data prevent us from deriving dissociation energies for the cluster ions.

Acknowledgments

We thank Prof. Stienkemeier, Freiburg, for his assistance and support in the construction of the He cluster source. F.Z. gratefully acknowledges a postdoctoral grant from Brazilian agency CNPq. This work has been partially supported by the FWF Wien, Austria, and the European Commission, Brussels.

References

[1] E.W. Becker, R. Klingerhofer, P. Lohse, Z. Naturforschg. 16a (1961) 1259.
[2] K.B. Whaley, Int. Rev. Phys. Chem. 13 (1994) 41.

[3] P. Sindzingre, D.M. Ceperley, M.L. Klein, Phys. Rev. Lett. 63 (1989) 1601.
[4] S. Grebenev, J.P. Toennies, A.F. Vilesov, Science 279 (1998) 2083.
[5] M. Farnik, J. Toennies, J. Chem. Phys. 122 (2005) 014307.
[6] F. Stienkemeier, A.F. Vilesov, J. Chem. Phys. 115 (2001) 10119.
[7] U. Henne, J.P. Toennies, J. Chem. Phys. 108 (1998) 9327.
[8] K. von Haeften, T. Laarmann, H. Wabnitz, T. Möller, Phys. Rev. Lett. 88 (2002) 233401.
[9] W. Schöllkopf, J.P. Toennies, Science 266 (1994) 1345.
[10] R. Briihl, R. Guardiola, A. Kalinin, O. Kornilov, J. Navarro, T. Savas, J. Toennies, Phys. Rev. Lett. 92 (2004) 185301.
[11] J. Gspann, H. Vollmar, J. Chem. Phys. 73 (1980) 1657.
[12] J. Gspann, Surf. Sci. 106 (1981) 219.
[13] H. Buchenau, J.P. Toennies, J. Northby, J. Chem. Phys. 95 (1991) 8134.
[14] M. Farnik, U. Henne, B. Samelin, J.P. Toennies, Z. Phys. D 40 (1997) 93.
[15] J.A. Northby, J. Chem. Phys. 115 (2001) 10065.
[16] B. von Issendorff, H. Haberland, R. Fröchtenicht, J.P. Toennies, Chem. Phys. Lett. 223 (1995) 23.
[17] P.W. Stephens, J.G. King, Phys. Rev. Lett. 51 (1983) 1538.
[18] N. Kobayashi, T. Kojima, Y. Kaneko, J. Phys. Soc. Jpn. 57 (1988) 1528.
[19] H. Buchenau, E.L. Knuth, J. Northby, J.P. Toennies, C. Winkler, J. Chem. Phys. 92 (1990) 6875.
[20] R. Fröchtenicht, U. Henne, J.P. Toennies, A. Ding, M. Fieber-Erdmann, T. Drewello, J. Chem. Phys. 104 (1996) 2548.
[21] B.E. Callicoatt, K. Förde, L.F. Jung, T. Ruchti, K.C. Janda, J. Chem. Phys. 109 (1998) 10195.
[22] T. Ruchti, K. Förde, B.E. Callicoatt, H. Ludwigs, K.C. Janda, J. Chem. Phys. 109 (1998) 10679.
[23] K. Gluch, S. Matt-Leubner, L. Michalak, O. Echt, A. Stamatovic, P. Scheier, T.D. Märk, J. Chem. Phys. 120 (2004) 2686.
[24] R.G. Cooks, J.H. Beynon, R.M. Caprioli, G.R. Lester, Metastable Ions, Elsevier, Amsterdam, 1973.
[25] K. Gluch, S. Matt-Leubner, O. Echt, R. Deng, J.U. Andersen, P. Scheier, T.D. Märk, Chem. Phys. Lett. 385 (2004) 449.
[26] T.D. Märk, P. Scheier, Chem. Phys. Lett. 137 (1987) 245.
[27] W. Miehle, O. Kandler, T. Leisner, O. Echt, J. Chem. Phys. 91 (1989) 5940.
[28] S. Prasalovich, K. Hansen, M. Kjellberg, V.N. Popok, E.E.B. Campbell, J. Chem. Phys. 123 (2005) 084317.
[29] O. Kandler, T. Leisner, O. Echt, E. Recknagel, Z. Phys. D 10 (1988) 295.
[30] O. Echt, O. Kandler, T. Leisner, W. Miehle, E. Recknagel, J. Chem. Soc. Faraday Trans. 86 (1990) 2411.
[31] J.M. Soler, N. Garcia, Phys. Rev. A 27 (1983) 3307.
[32] C.E. Klots, Phys. Rev. A 39 (1989) 339.
[33] T.P. Martin, Phys. Rep. 273 (1996) 199.
[34] W.A. DeHeer, Rev. Mod. Phys. 65 (1993) 611.
[35] C.E. Klots, J. Phys. Chem. 92 (1988) 5864.
[36] P.E. Barran, S. Firth, A.J. Stace, H.W. Kroto, K. Hansen, E.E.B. Campbell, Int. J. Mass Spectrom. Ion Process. 167/168 (1997) 127.
[37] C.E. Klots, Z. Phys. D 20 (1991) 105.
[38] J. Wilks, D.S. Betts, An Introduction to Liquid Helium, Clarendon Press, Oxford, 1987.
[39] C.E. Klots, Nature 327 (1987) 222.
[40] H. Haberland, B. von Issendorff, R. Fröchtenicht, J.P. Toennies, J. Chem. Phys. 102 (1995) 8773.
[41] T.F. Magnera, D.E. David, J. Michl, Chem. Phys. Lett. 123 (1986) 327.
[42] P. Scheier, T.D. Märk, Chem. Phys. Lett. 148 (1988) 393.
[43] T. Leisner, O. Echt, O. Kandler, X.Y. Yan, E. Recknagel, Chem. Phys. Lett. 148 (1988) 386.
[44] M. Foltin, G. Walder, A.W. Castleman, T.D. Märk, J. Chem. Phys. 94 (1991) 810.
[45] O. Echt, R. Parajuli, S. Matt, A. Stamatovic, P. Scheier, T.D. Märk, Chem. Phys. Lett. 361 (2002) 91.
[46] E. Scifoni, E. Bodo, G. Dellepiane, F.A. Gianturco, Eur. Phys. J. D 30 (2004) 363.
[47] M. Ovchinnikov, B. Grigorenko, K. Janda, V. Apkarian, J. Chem. Phys. 108 (1998) 9351.
[48] K. Hiraoka, T. Mori, J. Chem. Phys. 92 (1990) 4408.
[49] R.C. Dunbar, J. Chem. Phys. 90 (1989) 7369.
[50] K. Hansen, E.E.B. Campbell, Phys. Rev. E 58 (1998) 5477.
[51] T. Schindler, C. Berg, G. Niedner-Schatteburg, V. Bondybey, Chem. Phys. Lett. 250 (1996) 301.
[52] R. Parajuli, S. Matt, O. Echt, A. Stamatovic, P. Scheier, T.D. Märk, Chem. Phys. Lett. 352 (2002) 288.
[53] C.E. Klots, Z. Phys. D 21 (1991) 335.
[54] J.U. Andersen, E. Bonderup, K. Hansen, J. Chem. Phys. 114 (2001) 6518.